

Cite this: *Catal. Sci. Technol.*, 2020,  
10, 2994

# Computational investigation of the ligand effect on the chemo/regioselectivity and reactivity of cobalt-catalysed hydroformylation†

Pan Li,<sup>a</sup> Chaoren Shen,<sup>b</sup> Jie Min,<sup>a</sup> Jing-Yuan Mei,<sup>a</sup> Huan Zheng,<sup>bc</sup>  
Lin He<sup>b</sup> and Xinxin Tian<sup>a</sup>

The ligand effect on the chemo/regioselectivity and reactivity of cobalt-catalysed hydroformylation has been discussed. The results of the unmodified cobalt carbonyl catalyst showed that the regioselectivity of the terminal alkene substrate was mainly affected by the steric hindrance of the bulky alkyl substitution group and was insensitive to the elongation of the carbon chain. Regarding the addition of Co–H onto the alkene, modifying the cobalt carbonyl catalyst with a phosphine ligand led to more distinct differences between the Markovnikov and anti-Markovnikov pathways with respect to both the energy barrier and the reaction free energy. Among the four selected phosphines,  $\text{PBu}_3$  and  $\text{a}_5\text{-PhobPC}_5$  with large Tolman cone angles favoured anti-Markovnikov-type Co–H addition, which is beneficial for the generation of a linear product. The modification with phosphine also promoted the oxidative addition of  $\text{H}_2$  on the Co(I) centre by lowering the energy barrier of  $\text{H}_2$  splitting and generating a more stable Co(III)-dihydride complex but retarded the reductive elimination step by elevating its activation energy and reaction energy. On the whole, the hydroformylation mechanism is similar for both modified and unmodified cobalt carbonyl catalysts. Moreover,  $\text{PBu}_3$  modification on the catalyst does not intrinsically change the chemoselectivity of alkene but indeed improves the subsequent alcohol and formic ester formation.

Received 20th December 2019,  
Accepted 30th March 2020

DOI: 10.1039/c9cy02562f

rsc.li/catalysis

## Introduction

Hydroformylation, also known as the “oxo” process, is a well-established homogeneous catalytic reaction for manufacturing aldehydes from alkenes.<sup>1–8</sup> Various homogeneous catalysts with different transition-metal catalytic centres have been extensively explored.<sup>1–5</sup> Among them, rhodium and cobalt-based catalysts are two major options.<sup>1–8</sup> Although cobalt-based catalysts are less active than the rhodium analogues,<sup>1–5</sup> they possess the merits of earth abundance, low cost, and robustness towards poisons in the feedstock.<sup>5,6</sup> However, a primitive  $\text{HCo}(\text{CO})_4$  catalyst exhibits poor regioselectivity and requires a relatively high syngas pressure to avoid the decomposition of the cobalt carbonyl complex.<sup>5–8</sup> To meet the demand of high-pressure

conditions, reaction vessels with higher pressure limits are required to be used, which results in an increase in the production cost. On account of the linear and branched product mixture, the utilization of hydroformylation products is confined.<sup>7</sup> To improve these two defects, phosphine-modified cobalt carbonyl catalysts have been developed.<sup>8–14</sup> This alteration on the ligand not only enhances the stability and hydrogenation capability of the catalyst by the stronger electron-donating effect of the phosphine ligands, but also greatly elevates the selectivity towards the linear products due to the steric effect of the phosphine ligands.<sup>5–7</sup> Therefore, various bulky monophosphine ligands with stronger  $\sigma$ -electron-donor strength, less  $\pi$ -acid character, or large Tolman cone angle<sup>15–17</sup> (e.g.,  $\text{PBu}_3$ , phobanes, Lim, VCH, and PA ligand family<sup>18–25</sup>) have been evaluated in cobalt-catalysed alkene hydroformylation. Lower syngas pressure conditions and better regioselectivity have been achieved.<sup>26</sup> In contrast to the lasting and intensive experimental investigations on cobalt-catalysed hydroformylation<sup>7,27–32</sup> as well as the progressive theoretical studies on the phosphine ligand effect on rhodium-catalysed hydroformylation,<sup>33–38</sup> the computational mechanistic studies on cobalt-catalysed hydroformylation are still mostly focused on the original phosphine-free cobalt carbonyl catalyst.<sup>33,34,39–51</sup> The

<sup>a</sup> Institute of Molecular Science, Key Laboratory of Materials for Energy Conversion and Storage of Shanxi Province, Shanxi University, Taiyuan 030006, P. R. China. E-mail: tianxx@sxu.edu.cn

<sup>b</sup> State Key Laboratory for Oxo Synthesis and Selective Oxidation, Suzhou Research Institute of LICP, Lanzhou Institute of Chemical Physics (LICP), Chinese Academy of Sciences, Lanzhou 730000, P. R. China. E-mail: shenchaoren@licp.cas.cn, shenchaoren@gmail.com

<sup>c</sup> University of Chinese Academy of Sciences, Beijing 100039, P. R. China

† Electronic supplementary information (ESI) available. See DOI: 10.1039/c9cy02562f

mechanism involves different unsaturated hydrocarbon substrates,<sup>39–43</sup> hydrogen splitting, and reductive elimination steps in hydroformylation<sup>44</sup> and kinetics.<sup>45,46</sup> Automated methods have also been exploited.<sup>47–51</sup> However, as an important factor to regulate reactivity and regioselectivity, the ligand effect on cobalt-catalysed hydroformylation has not been quantitatively investigated by density functional theory (DFT) computations.

According to the widely accepted Heck–Breslow mechanism,<sup>7,52,53</sup> cobalt-catalysed hydroformylation process generally consists of five steps (Fig. 1): i) formation of a  $\pi$ -complex between the unsaturated  $\text{HCo}(\text{CO})_2\text{L}$  complex and the alkene substrate; ii) generation of cobalt-alkyl complex *via* the addition of Co–H into the alkene; iii) formation of the cobalt-acyl complex through migratory CO insertion; iv) the oxidative splitting of  $\text{H}_2$  on cobalt; v) release of the aldehyde and regeneration of  $\text{HCo}(\text{CO})_2\text{L}$  by way of reductive elimination. During this reaction process, the regioselectivity of hydroformylation is decided by the Co–H addition step. Also, the electric properties of the ligand on the cobalt catalyst has distinct effects on each step of the process. Understanding the electronic and steric effects of the ligand on these steps would further help in improving the activity and regioselectivity of the cobalt catalysts. Although great advances have been made in experimental technique, it is still challenging to monitor the transient intermediates due to their instability.<sup>19,24,54–62</sup> Theoretical computation based on DFT is a complementary but more accessible tool to solve such issues and DFT results can help to get a thorough insight into the mechanism of the reaction process.<sup>63,64</sup> Herein, the phosphine ligand effect on the reactivity and selectivity of cobalt-catalysed hydroformylation was investigated based on the computational research. We performed a systematic study on all the steps in the Heck–Breslow mechanism and the side reactions of the  $\text{PBu}_3$ -modified cobalt carbonyl catalyst. Considering the diverse

and changeable configuration of cobalt-alkyl and cobalt-acyl complexes bearing phosphine ligand as well as the complicated interconversion between them, only the reaction steps involving cobalt hydride intermediates of other phosphine ligands were studied.

## Computational methods

Considering the applicability of M06 hybrid meta exchange–correlation functional<sup>65</sup> in homogeneous organometallic thermochemistry,<sup>66,67</sup> geometry optimizations were conducted with the M06 functional. The Stuttgart–Dresden basis set was used for the cobalt atom<sup>68,69</sup> and the 6-311+G(d) basis set was used for the other atoms. Vibrational frequencies were calculated to verify all the stationary points as the minima (no imaginary frequency) or transition state (TS, only one imaginary frequency). Intrinsic reaction coordinate (IRC) calculations were also conducted to confirm that each transition state connects two relevant minima. Free energies (in  $\text{kcal mol}^{-1}$ ) at 298.15 K and 1 atm were used in the following discussions. Steric maps were analysed by SambVca 2 web tool.<sup>70</sup> All other calculations were performed on the Gaussian 09 package.<sup>71</sup>

The following notations are employed to represent the different types of complexes involved in each elementary reaction throughout the text. **a**, **b**, **c**, and **d** represent the isomers of the  $\pi$ -complex  $\text{HCo}(\eta^2\text{-alkene})(\text{CO})_2\text{L}$  ( $\text{L} = \text{CO}$  or phosphine ligand); **e**, **f**, **g**, and **h** represent the isomers of  $\text{Co}(\eta^2\text{-alkyl})(\text{CO})_2\text{L}$ ; **i** and **j** represent the isomers of  $\text{Co}(\eta^1\text{-C}_3\text{H}_7)(\text{CO})_4$  or  $\text{Co}(\eta^1\text{-C}_3\text{H}_7)(\text{CO})_3(\text{PBu}_3)$ ; **k**, **l**, **m**, and **n** represent the isomers of  $(\eta^2\text{-C}_3\text{H}_7\text{CO})\text{Co}(\text{CO})_2(\text{PBu}_3)$ ; **o** represents  $\text{Co}(\eta^1\text{-}n\text{-C}_3\text{H}_7)(\text{CO})_3$ ; **p** and **q** represent the isomers of the  $\pi$ -complex  $\text{HCo}(\eta^2\text{-C}_3\text{H}_7\text{CHO})(\text{CO})_3$  or  $\text{HCo}(\eta^2\text{-C}_3\text{H}_7\text{CHO})(\text{CO})_2(\text{PBu}_3)$ ; **r** and **v** represent  $[\eta^2\text{-C}_3\text{H}_7\text{CH}(\text{OH})]\text{Co}(\text{CO})_3$  or  $[\eta^2\text{-C}_3\text{H}_7\text{CH}(\text{OH})]\text{Co}(\text{CO})_2(\text{PBu}_3)$ ; **s** represents  $(\eta^1\text{-C}_3\text{H}_7\text{CH}_2\text{O})\text{Co}(\text{CO})_3$  or  $(\eta^1\text{-C}_3\text{H}_7\text{CH}_2\text{O})\text{Co}(\text{CO})_2(\text{PBu}_3)$ ; **t** represents  $(\eta^1\text{-C}_3\text{H}_7\text{CH}_2\text{O})\text{Co}(\text{CO})_4$  or  $(\eta^1\text{-C}_3\text{H}_7\text{CH}_2\text{O})\text{Co}(\text{CO})_3(\text{PBu}_3)$ ; **u** represents  $(\eta^1\text{-C}_4\text{H}_9\text{OCO})\text{Co}(\text{CO})_3$  or  $(\eta^1\text{-C}_4\text{H}_9\text{OCO})\text{Co}(\text{CO})_2(\text{PBu}_3)$ . The notations **ma** and **anti-ma** respectively represent Markovnikov and anti-Markovnikov hydroformylation pathway. The notations **alkane**, **alcohol**, and **formate** respectively represent the pathways of alkene hydrogenation to alkane, aldehyde reduction to alcohol, and carbonylative reduction of aldehyde to formic ester. The subscripts respectively represent the following transformations: i) **rotate** refers to the C=C or C=O bond rotation, **acyl-rotate** refers to the rotation of the butyryl group, **alkyl-rotate** refers to the rotation of the propyl group; ii) **add** refers to Co–H addition; iii) **iso** refers to the isomerization of the cobalt-alkyl complexes, **acyl-iso** refers to the isomerization of the cobalt-acyl complexes; iv) **CO** refers to the addition of the carbonyl ligand, **H2** refers to the addition of the  $\text{H}_2$  molecule; vi) **insert** refers to migratory CO insertion; vii) **splitting** refers to hydrogen splitting; viii) **eliminate** refers to reductive elimination.  $\Delta G$  represents the relative free energy with respect to conformation **a**;  $\Delta G_A$  and

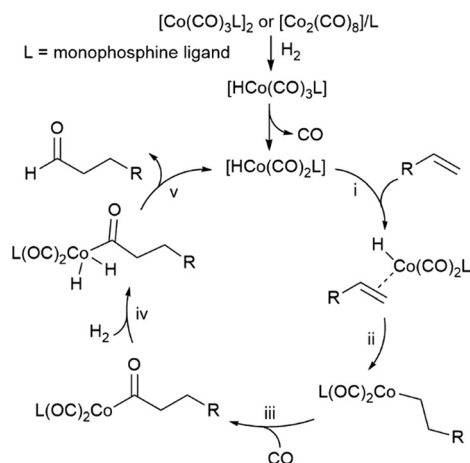


**Fig. 1** Simplified Heck–Breslow mechanism (the scenario of regioselectivity towards the branched product is omitted for clarity) of olefin hydroformylation catalysed by phosphine-modified cobalt carbonyl catalyst.

**Table 1** Newman projection and relative free energy ( $\Delta G$ , kcal mol<sup>-1</sup>) of HCo( $\eta^2$ -alkene)(CO)<sub>2</sub>L with different perpendicular olefin coordination conformations at the equatorial site

Entry	<b>a</b>	<b>b</b>	$\Delta G^c$
1			0.6
2 <sup>a</sup>			0.1
3			<0.1
4			0.1
5			0.8
6			0.2
7 <sup>b</sup>			0.1
8			0.1

<sup>a</sup> R = 2,4-dimethylpentyl. <sup>b</sup> L1 = a<sub>5</sub>-PhobPC<sub>5</sub>. <sup>c</sup>  $\Delta G = G(\mathbf{b}) - G(\mathbf{a})$ .

$\Delta G_R$  represent the activation energy and reaction free energy of the elementary step, respectively.

## Results and discussion

### Co-H addition of unmodified HCo(CO)<sub>3</sub>

Firstly, the Co-H addition of unmodified HCo(CO)<sub>3</sub> on propylene, 4,6-dimethyl-1-heptene (one of the components in the tripropylene mixture), isobutene, and 2,4,4-trimethyl-1-pentene (the major isomer of the diisobutene mixture) were investigated. Consistent with the previous reports,<sup>72-75</sup> there are two orientations for C=C bond coordination with the cobalt centre of HCo(CO)<sub>3</sub> in the  $\pi$ -complexes of HCo( $\eta^2$ -alkene)(CO)<sub>3</sub>: the double bond is perpendicular or parallel to the axial Co-H bond. In the case of these four alkenes, the perpendicular conformation is more stable than the parallel

conformation. There are two different kinds of perpendicular conformations for propene, 4,6-dimethyl-1-heptene, and 2,4,4-trimethyl-1-pentene: methyl, 2,4-dimethylpentyl, or 2,2-dimethylpropyl group is located at the same or opposite side of the Co-H bond. In these cases, the free energy differences between these two kinds of perpendicular conformation are all much less than 1 kcal mol<sup>-1</sup> (entries 1-3 of Table 1), which are most likely within the error of DFT computations. For the purpose of simplifying the discussion of the reaction mechanism, the conformations **a** were selected as the starting point to investigate the Co-H addition of HCo(CO)<sub>3</sub>. For propene or isobutene, the formation of **a** through coordination with HCo(CO)<sub>3</sub> is a weakly exothermic elementary reaction. But with the change in alkene from propene/isobutene to 4,6-dimethyl-1-heptene/2,4,4-trimethyl-1-pentene, the exothermic nature of the reaction becomes much more significant. For detailed results, see Table S1 in ESI.†

The most stable perpendicular conformations **a** were firstly transformed to **c** or **d** through the rotation of the C=C bond. Afterwards, *via* the migration of the hydrogen atom from cobalt onto the C=C bond of these four alkenes, the  $\pi$ -complexes HCo( $\eta^2$ -alkene)(CO)<sub>3</sub> **c/d** were converted to the corresponding complexes Co( $\eta^1$ -alkyl)(CO)<sub>3</sub> **e/f** with an additional Co...H-C agostic interaction at the formally vacant equatorial position. The free energy changes due to Co-H addition onto the four chosen alkenes are summarized in Table 2. The Co-H addition along Markovnikov (**a** → **e**) and anti-Markovnikov (**a** → **f**) pathways is exothermic for propene and isobutene but endothermic for 4,6-dimethyl-1-heptene and 2,4,4-trimethyl-1-pentene. The comparison between propene and 4,6-dimethyl-1-heptene as well as between isobutene and 2,4,4-trimethyl-1-pentene exhibits that the energy barrier of C=C bond rotation is significantly elevated and this step becomes much more endothermic after elongation of the carbon chain or enlargement of the substitution group. However, the activation energy and reaction free energy change of the Co-H addition step were much less impacted. In the cases of propene, 4,6-dimethyl-1-heptene, and isobutene, the energy differences in  $\Delta G_A$  and  $\Delta G_R$  for C=C bond rotation and Co-H addition between Markovnikov and anti-Markovnikov pathway were less than 1 kcal mol<sup>-1</sup>. Even the energy differences between the two final states of the Co-H addition process (**e** and **f**) were less than 0.5 kcal mol<sup>-1</sup>. Only in the case of 2,4,4-trimethyl-1-pentene, the anti-Markovnikov pathway is notably more thermodynamic-favoured than the Markovnikov pathway by about 3.5 kcal mol<sup>-1</sup>.

The energy patterns for the Co-H addition of the unmodified cobalt carbonyl catalyst onto isobutene, 4,6-dimethyl-1-heptene, isobutene, and 2,4,4-trimethyl-1-pentene indicate that the hydroformylation regioselectivity of the mono-substituted terminal alkene substrate is insensitive to the elongation of the aliphatic chain. For di-substituted terminal aliphatic alkene substrates, the bulky steric hinderance provided by the alkyl substitution can make the anti-Markovnikov pathway more beneficial.

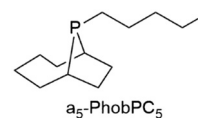
**Table 2** Free energy changes for the Co–H addition of  $\text{HCo}(\text{CO})_3$  onto propene, 4,6-dimethyl-1-heptene, isobutene, and 2,4,4-trimethyl-1-pentene with different regioselectivities (values are in  $\text{kcal mol}^{-1}$ )

Markovnikov pathway					
Entry	R <sup>1</sup> /R <sup>2</sup>	$\Delta G(\text{TS}_{\text{rotate}})$	$\Delta G(\text{c})$	$\Delta G(\text{TS}_{\text{add-ma}})/\Delta G_{\text{A}}$	$\Delta G(\text{e})/\Delta G_{\text{R}}$
1	CH <sub>3</sub> /H	5.5	3.4	6.3/2.9	-3.3/-6.7
2	2,4-dimethylpentyl/H	20.2	17.1	19.9/2.8	10.9/-6.2
3	CH <sub>3</sub> /CH <sub>3</sub>	4.1	1.3	5.6/4.3	-1.8/-3.1
4	CH <sub>3</sub> /CH <sub>2</sub> C(CH <sub>3</sub> ) <sub>2</sub>	18.9	16.1	20.6/4.5	15.5/-0.6
Anti-Markovnikov pathway					
Entry	R <sup>1</sup> /R <sup>2</sup>	$\Delta G(\text{TS}_{\text{rotate}})$	$\Delta G(\text{d})$	$\Delta G(\text{TS}_{\text{add-anti-ma}})/\Delta G_{\text{A}}$	$\Delta G(\text{f})/\Delta G_{\text{R}}$
5	CH <sub>3</sub> /H	4.9	3.5	6.1/2.6	-3.1/-6.6
6	2,4-dimethylpentyl/H	19.4	17.8	20.1/2.3	11.0/-6.8
7	CH <sub>3</sub> /CH <sub>3</sub>	3.8	1.7	5.6/3.9	-2.0/-3.7
8	CH <sub>3</sub> /CH <sub>2</sub> C(CH <sub>3</sub> ) <sub>2</sub>	18.1	16.5	20.5/4.0	12.4/-4.1

### Co–H addition of phosphine-modified cobalt carbonyl catalysts

Four kinds of phosphines, namely,  $\text{PH}_3$ ,  $\text{PMe}_3$ ,  $\text{PBu}_3$ , and *n*-pentyl-9-phosphabicyclo[4.2.1]nonane ( $a_5\text{-PhobPC}_5$ , Fig. 2) were selected as the model ligands to investigate the ligand effect on the regioselectivity during the cobalt-catalysed hydroformylation with propene. Considering that coordination-unsaturated  $\text{HCo}(\text{CO})_2\text{L}$  with 16 valence electrons obtained *via* CO dissociation from  $\text{HCo}(\text{CO})_3\text{L}$  is generally regarded as the active species of the cobalt hydroformylation catalyst, the thermodynamics for the formation of the phosphine-modified pre-catalyst was investigated. According to the previous computational research,<sup>76</sup> equatorial CO dissociation was energetically more favoured than axial CO dissociation in  $\text{HCo}(\text{CO})_4$ . Therefore, the free-energy changes for the conversion from  $\text{HCo}(\text{CO})_4$  to  $\text{HCo}(\text{CO})_3\text{L}$  ( $\text{L}$  = phosphine ligand) *via* ligand exchange on the equatorial site were computed. It was found that except for the case of  $\text{PH}_3$ , the substitution of equatorial carbonyl ligand by  $\text{PMe}_3$ ,  $\text{PBu}_3$ , or  $a_5\text{-PhobPC}_5$  was thermodynamically favored (for detailed results, see Table S2 in ESI<sup>†</sup>). Also, compared with the equatorial CO dissociation on  $\text{HCo}(\text{CO})_4$  to form the active species  $\text{HCo}(\text{CO})_3$ , the corresponding process on  $\text{HCo}(\text{CO})_3\text{L}$  became more endothermic (for details,

see Table S3 in the ESI<sup>†</sup>), except for the  $a_5\text{-PhobPC}_5$ -substituted cobalt carbonyl hydride complex, which turns out to be less endothermic. A similar trend was also found in the CO dissociation process of  $\text{Co}(\text{CO})_3\text{L}(\text{COR})$ , which is attributed to the steric effects of  $a_5\text{-PhobPC}_5$  by Birbeck *et al.*<sup>24</sup> We also compared the preference of phosphine substitution between the axial and equatorial sites of  $\text{HCo}(\text{CO})_2\text{L}$  by the relative free energy and enthalpy (for detailed results, see Table S4 in the ESI<sup>†</sup>). Similar to the previous computational results,<sup>77</sup> the monodentate phosphine ligands prefer equatorial substitution. Based on these results and in order to simplify the model for computational survey, only the scenarios of the  $\text{HCo}(\text{CO})_2\text{L}$  complex with phosphine substitution at the equatorial position were considered. The detailed free energy changes for the coordination of propene or isobutene with  $\text{HCo}(\text{CO})_2\text{L}$

**Fig. 2** Structure of *n*-pentyl-9-phosphabicyclo[4.2.1]nonane ( $a_5\text{-PhobPC}_5$ ).

are provided in Table S1 of the ESI.† When propene is coordinated to the  $\text{HCo}(\text{CO})_2\text{L}$  catalyst with phosphine substitution at the equatorial position, the perpendicular conformation is more stable than the parallel conformation. Also, for the perpendicular conformations, similar to that of  $\text{HCo}(\eta^2\text{-alkene})(\text{CO})_3$ , the more stable **a** conformation with the methyl group of propene on the opposite side of the Co–H bond was chosen as the starting point, even though the energy differences between **a** and **b** are less than 1 kcal mol<sup>-1</sup> (entries 4–7 of Table 1). Owing to the presence of the phosphine ligand, the isomerization of  $\text{Co}(\eta^2\text{-C}_3\text{H}_7)(\text{CO})_2\text{L}$  from *cis* configuration to *trans* configuration (**e** → **g**; **f** → **h**) was also considered to demonstrate the probable

transformation on the cobalt-alkyl complexes. The detailed energy changes for the rotation–addition–isomerization process are summarized in entries 1–8 of Table 3. The results for the small energy differences in the C=C bond rotation barrier/reaction energy of  $\text{HCo}(\eta^2\text{-alkene})(\text{CO})_3$  between Markovnikov and anti-Markovnikov pathways verify that the transformation between parallel and perpendicular conformation is very easy and has negligible effect on the reaction. Therefore, the C=C bond rotation step is not discussed in the following part but the corresponding data are listed out for completeness.

Although  $\text{PH}_3$  has strong electron-donating ability, its steric hindrance is relatively less than that of any other

**Table 3** Free energy changes for the Co–H addition of  $\text{HCo}(\text{CO})_2\text{L}$  onto propene and isobutene with different regioselectivities (values are in kcal mol<sup>-1</sup>, R = H or Me)

Markovnikov pathway of propene (R = H)							
Entry	L	$\Delta G(\text{TS}_{\text{rotate-ma}})$	$\Delta G(\text{c})$	$\Delta G(\text{TS}_{\text{add-ma}})/\Delta G_{\text{A}}$	$\Delta G(\text{e})/\Delta G_{\text{R}}$	$\Delta G(\text{TS}_{\text{iso-ma}})/\Delta G_{\text{A}}$	$\Delta G(\text{g})/\Delta G_{\text{R}}$
1	$\text{PH}_3$	7.2	4.4	5.3/0.9	-1.5/-5.9	4.1/5.3	-2.0/-0.5
2	$\text{PMe}_3$	6.5	5.0	7.6/2.6	1.5/-3.4	5.7/4.2	-1.7/-3.2
3	$\text{PBu}_3$	8.2	4.5	9.8/5.3	4.5/0.0	5.1/0.6	-3.4/-7.9
4	$\text{a}_5\text{-PhobPC}_5$	7.1	3.5	7.2/3.7	—	—	-2.3/-5.8
Anti-Markovnikov pathway of propene (R = H)							
Entry	L	$\Delta G(\text{TS}_{\text{rotate-anti-ma}})$	$\Delta G(\text{d})$	$\Delta G(\text{TS}_{\text{add-anti-ma}})/\Delta G_{\text{A}}$	$\Delta G(\text{f})/\Delta G_{\text{R}}$	$\Delta G(\text{TS}_{\text{iso-anti-ma}})/\Delta G_{\text{A}}$	$\Delta G(\text{h})/\Delta G_{\text{R}}$
5	$\text{PH}_3$	5.3	4.0	4.6/0.6	-2.2/-6.2	4.1/6.3	-2.3/-0.1
6	$\text{PMe}_3$	5.6	5.1	7.2/2.1	-1.1/-6.2	7.3/8.4	-1.3/-0.2
7	$\text{PBu}_3$	6.6	5.6	8.5/2.9	2.6/-3.0	7.6/5.0	-3.4/-6.0
8	$\text{a}_5\text{-PhobPC}_5$	7.5	6.9	7.5/0.6	-3.5/-10.4	—	—
Markovnikov pathway of isobutene (R = Me)							
Entry	L	$\Delta G(\text{TS}_{\text{rotate-ma}})$	$\Delta G(\text{c})$	$\Delta G(\text{TS}_{\text{add-ma}})/\Delta G_{\text{A}}$	$\Delta G(\text{e})/\Delta G_{\text{R}}$	$\Delta G(\text{TS}_{\text{iso-ma}})/\Delta G_{\text{A}}$	$\Delta G(\text{g})/\Delta G_{\text{R}}$
9	$\text{PH}_3$	5.3	2.6	5.9/3.3	-1.1/-3.7	3.3/4.4	-1.8/-0.7
10	$\text{PMe}_3$	4.4	3.3	7.5/4.2	2.1/-1.2	4.2/2.1	-2.1/-4.2
11	$\text{PBu}_3$	7.9	4.2	10.3/6.1	—	—	-1.9/-6.1
Anti-Markovnikov pathway of isobutene (R = Me)							
Entry	L	$\Delta G(\text{TS}_{\text{rotate-anti-ma}})$	$\Delta G(\text{d})$	$\Delta G(\text{TS}_{\text{add-anti-ma}})/\Delta G_{\text{A}}$	$\Delta G(\text{f})/\Delta G_{\text{R}}$	$\Delta G(\text{TS}_{\text{iso-anti-ma}})/\Delta G_{\text{A}}$	$\Delta G(\text{h})/\Delta G_{\text{R}}$
12	$\text{PH}_3$	6.3	4.0	5.0/1.0	-1.0/-5.0	5.0/6.0	-0.6/0.4
13	$\text{PMe}_3$	4.7	4.2	6.6/2.4	0.0/-4.2	6.5/6.5	-3.2/-3.2
14	$\text{PBu}_3$	8.3	6.3	10.4/4.1	—	—	-2.0/-8.3

tertiary-alkyl phosphine ligand.<sup>15</sup> As shown in Table 3, the Co–H addition barrier of the complexes with PH<sub>3</sub> ligand are considerably lower than those of the complexes with PMe<sub>3</sub>, PBu<sub>3</sub>, and a<sub>5</sub>-PhobPC<sub>5</sub>. Furthermore, compared with unmodified cobalt carbonyl complex, the presence of PH<sub>3</sub> ligand considerably diminishes the energy barrier of migratory Co–H insertion into the C=C bond to generate the Co(η<sup>2</sup>-C<sub>3</sub>H<sub>7</sub>) complex (0.9/0.6 vs. 2.9/2.6 kcal mol<sup>-1</sup>). After Co–H addition, PH<sub>3</sub> is still at the equatorial position in the Co(η<sup>2</sup>-C<sub>3</sub>H<sub>7</sub>) complexes **e** and **f**. Then, they undergo isomerization to the more stable Co(η<sup>2</sup>-C<sub>3</sub>H<sub>7</sub>)(CO)<sub>2</sub>(PH<sub>3</sub>) isomers **g** and **h** with (iso)propyl at the trans position of PH<sub>3</sub> respectively *via* the energy barrier of 5.6 kcal mol<sup>-1</sup> from **e** to **g** and 6.3 kcal mol<sup>-1</sup> from **f** to **h**. Comparing the free energy changes of the whole rotation–addition–isomerization process between HCo(CO)<sub>2</sub>(PH<sub>3</sub>) and HCo(CO)<sub>3</sub>, we can see that the substitution of the carbonyl ligand with PH<sub>3</sub> makes the anti-Markovnikov pathway more kinetically and thermodynamically favoured.

The results of PMe<sub>3</sub> and PBu<sub>3</sub> more obviously demonstrate the ligand effect on the regioselectivity of hydroformylation. In the Co–H addition step, when the phosphine ligand at the equatorial site is PMe<sub>3</sub>, the energy barrier in the anti-Markovnikov pathway is 0.5 kcal mol<sup>-1</sup> lower than that in the Markovnikov pathway and the anti-Markovnikov pathway is more exothermic than the Markovnikov pathway by about 2.8 kcal mol<sup>-1</sup>. The similar process and energy patterns are also manifested in the case of PBu<sub>3</sub>. The energy barrier for the Co–H addition step in the anti-Markovnikov pathway is 2.4 kcal mol<sup>-1</sup> lower than that in the Markovnikov pathway and the anti-Markovnikov pathway is more exoergic than the Markovnikov pathway by about 3.0 kcal mol<sup>-1</sup>. The results indicate that introducing PMe<sub>3</sub> and PBu<sub>3</sub> ligands makes the anti-Markovnikov pathway more advantageous than the Markovnikov pathway, which leads to the linear selectivity of the hydroformylation product. According to the reported experimental results,<sup>12–14</sup> modifying the cobalt carbonyl catalyst with PBu<sub>3</sub> largely improved the regioselectivity towards linear products in the cobalt-catalysed hydroformylation of 1-pentene and propene. The obtained energy patterns verify that PBu<sub>3</sub> improves the regioselectivity by the contributing in the Co–H addition step. Our computation results also demonstrate that the isomerization of Co(η<sup>2</sup>-C<sub>3</sub>H<sub>7</sub>)(CO)<sub>2</sub>L (L = PH<sub>3</sub>, PMe<sub>3</sub> or PBu<sub>3</sub>) from *cis* to the more stable *trans* isomer can occur after Co–H addition driven by the thermodynamic preference and low barrier.

a<sub>5</sub>-PhobPC<sub>5</sub> belongs to a large family of bicyclic tertiary phosphine ligands known as phobanes (9-phosphabicyclononanes including [3.3.1] isomers and [4.2.1] isomers).<sup>21</sup> As more stable and less volatile phosphines than simple trialkylphosphines, they were also developed for the phosphine-modified cobalt-catalysed hydroformylation by Shell.<sup>18</sup> Tolman cone angle parameters of these phobanes range from 159 to 175°,<sup>21–23</sup> which are even larger than that of PBu<sub>3</sub> (132°). The electron donor strength of a<sub>5</sub>-PhobPC<sub>5</sub> is comparable to that of PBu<sub>3</sub>;<sup>24,78</sup> thus, a<sub>5</sub>-PhobPC<sub>5</sub> can be

regarded as a PBu<sub>3</sub>-like ligand with similar electronic properties. When using phoban derivatives as the ligand, linear aldehyde and alcohol are the major products.<sup>21</sup> Our computational results disclose some features of a<sub>5</sub>-PhobPC<sub>5</sub> in this rotation–addition process. In the Markovnikov pathway, after surmounting the energy barrier of Co–H addition, the reaction directly generates the Co(η<sup>2</sup>-i-C<sub>3</sub>H<sub>7</sub>)(CO)<sub>2</sub>(a<sub>5</sub>-PhobPC<sub>5</sub>) complex **g** with phosphine at the *trans* position of the isopropyl group. In the anti-Markovnikov addition pathway, the generated Co(η<sup>1</sup>-*n*-C<sub>3</sub>H<sub>7</sub>)(CO)<sub>2</sub>(a<sub>5</sub>-PhobPC<sub>5</sub>) complex **f** with phosphine at the equatorial site has no Co⋯H–C agostic interaction at the formally vacant equatorial position due to the steric hinderance of a<sub>5</sub>-PhobPC<sub>5</sub>. Thus, the isomerization from complex **f** to **h** was omitted. It can be seen that the activation energies of the Co–H addition step in the anti-Markovnikov pathway are about 3.1 kcal mol<sup>-1</sup> lower than that in the Markovnikov pathway. Moreover, the Co–H addition step in the anti-Markovnikov pathway is much more exothermic than in the Markovnikov pathway by about 4.6 kcal mol<sup>-1</sup>. Both the much lower activation energy and the thermodynamic advantage of the anti-Markovnikov Co–H addition step leads to the higher preference of the linear product.

Then, the ligand effect on the regioselectivity of isobutene substrate was also investigated. The rotation–addition process of isobutene on the phosphine-modified cobalt carbonyl complex is similar to the process of propene (entries 9–14 of Table 3). It is noteworthy that the most stable perpendicular conformation of HCo(η<sup>2</sup>-isobutene)(CO)<sub>2</sub>(PH<sub>3</sub>) is that with two methyl groups adjacent to PH<sub>3</sub> instead of that with the methyl groups on the opposite side of the phosphine ligand (entry 8 of Table 1). In comparison with the results of the unmodified cobalt carbonyl catalyst, introducing PH<sub>3</sub> and PMe<sub>3</sub> at the equatorial site enlarges the gap in the activation energy (0.4 vs. 2.3/1.8 kcal mol<sup>-1</sup>) and the reaction free energy (0.6 vs. 1.3/3.0 kcal mol<sup>-1</sup>) of the Co–H addition step between the Markovnikov pathway and the anti-Markovnikov pathway, which makes the anti-Markovnikov pathway more favored. According to the previous report,<sup>12</sup> when isobutene is the substrate, the HCo(CO)<sub>2</sub>(PBu<sub>3</sub>) moiety was added exclusively to the terminal position of isobutene. The computational results disclose that the Co–H addition step in the Markovnikov pathway has about 2.0 kcal mol<sup>-1</sup> higher activation energy and is about 2.2 kcal mol<sup>-1</sup> less exothermic than that in the anti-Markovnikov pathway. From these traits, we rationally infer that the regioselectivity of isobutene on the PBu<sub>3</sub>-modified cobalt carbonyl catalyst is mainly controlled by the Co–H addition step.

With respect to the regioselectivity of propene and isobutene, the results in Table 3 display a qualitative correlation between the energy barrier (or reaction free energy) and Tolman cone angle of the phosphines. A larger Tolman cone angle (PH<sub>3</sub> < PMe<sub>3</sub> < PBu<sub>3</sub> < a<sub>5</sub>-PhobPC<sub>5</sub>)<sup>16,21,24</sup> enlarges the difference in the energy barrier between the Markovnikov and the anti-Markovnikov pathway and makes the anti-Markovnikov pathway more kinetically favoured. To

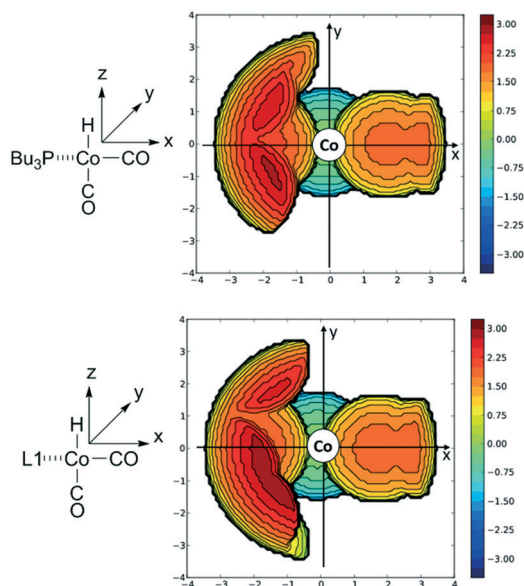


Fig. 3 Steric maps of  $\text{HCo}(\text{CO})_2(\text{PBu}_3)$  and  $\text{HCo}(\text{CO})_2(\text{a}_5\text{-PhobPC}_5)$  around the cobalt centre (units of cartesian coordinates are in angstrom).

analyse the steric environment around the cobalt centre, the topographic steric maps of  $\text{HCo}(\text{CO})_2(\text{PBu}_3)$  and  $\text{HCo}(\text{CO})_2(\text{a}_5\text{-PhobPC}_5)$  complexes were plotted, as shown in Fig. 3. The steric maps show that owing to the bulky volume of  $\text{a}_5\text{-PhobPC}_5$  and  $\text{PBu}_3$ , both the upper-left quadrant and lower-left quadrant of the cross-section around the cobalt centre are heavily occupied by the phosphine ligand. The space occupied by  $\text{a}_5\text{-PhobPC}_5$  in these two quadrants is even larger than that by  $\text{PBu}_3$ . The congestion of the left quadrants around cobalt in the  $\pi$ -complex  $\text{HCo}(\eta^2\text{-alkene})(\text{CO})_2\text{L}$  confines the orientation of the coordinated alkene and the rotation direction of the  $\text{C}=\text{C}$  bond on the cobalt centre as well as controls the regioselectivity of the following  $\text{Co-H}$  addition onto the  $\text{C}=\text{C}$  bond, which distinguishes the anti-Markovnikov pathway from the Markovnikov pathway.

The behaviour of  $\text{a}_5\text{-PhobPC}_5$  in the  $\text{Co-H}$  addition process is rather different from that of  $\text{PBu}_3$ , though both have a large Tolman cone angle. The equatorial  $\text{CO}$  dissociation from  $\text{HCo}(\text{CO})_3(\text{a}_5\text{-PhobPC}_5)$  to generate the active species is less endothermic than from either  $\text{HCo}(\text{CO})_3(\text{PBu}_3)$  or  $\text{HCo}(\text{CO})_4$ . One of the features of  $\text{a}_5\text{-PhobPC}_5$  is its unsymmetrical structure. To achieve the high hydroformylation activity of  $\text{HCo}(\text{CO})_4$  but to still maintain the good stability, bicyclic tertiary phosphine ligand adopting an unsymmetrical structure may be a potential choice to achieve both high activity and regioselectivity.

#### Potential energy profiles for the Markovnikov and anti-Markovnikov processes on the $\text{PBu}_3$ -modified cobalt carbonyl catalyst

To get a full understanding of the linear selectivity of hydroformylation on the terminal alkenes by phosphine-

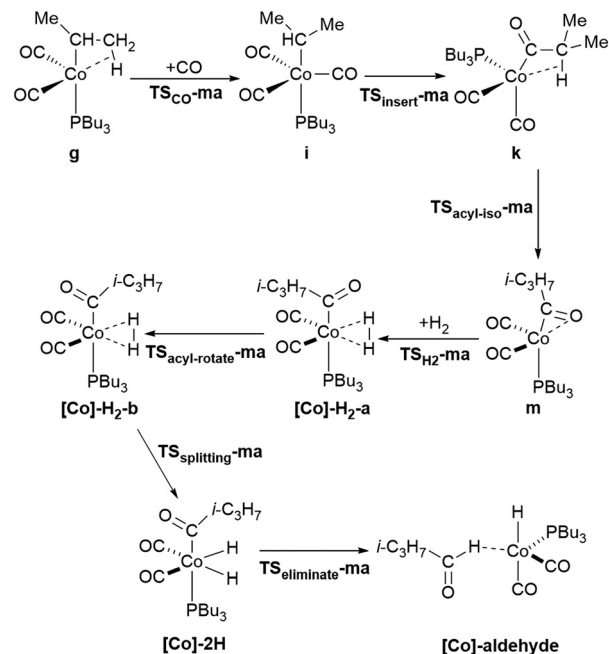


Fig. 4 The transformation pathway from **g** to **[Co]-aldehyde** after Markovnikov addition.

modified cobalt carbonyl catalyst, the comparison of potential energy profiles between the linear-selective and branch-selective propene hydroformylation processes on the  $\text{PBu}_3$ -modified cobalt carbonyl catalyst was made. The evolution from **g/h** to the corresponding **[Co]-aldehyde** was therefore studied. As shown in Fig. 4, the transformation from **g** to **[Co]-aldehyde** undergoes the following four elementary reactions: i) breaking the agostic ( $\text{Co}\cdots\text{H}-\text{C}$ ) interaction and adding the carbonyl ligand onto the  $\text{Co}$  centre of **g** via  $\text{TS}_{\text{Co-ma}}$  to afford the  $\text{Co}(\eta^1\text{-C}_3\text{H}_7)(\text{CO})_3(\text{PBu}_3)$  complexes **i**, in which the *i*-propyl group is at the trans position of  $\text{PBu}_3$ ; ii) the migratory  $\text{CO}$  insertion of **i** via  $\text{TS}_{\text{insert-ma}}$  to generate the  $(\eta^2\text{-C}_3\text{H}_7\text{CO})\text{Co}(\text{CO})_2(\text{PBu}_3)$  complex **k** with the propyl group at the *cis* position of  $\text{PBu}_3$  and containing the agostic ( $\text{Co}\cdots\text{H}-\text{C}$ ) interaction at the equatorial site; iii) the isomerization of **k** via  $\text{TS}_{\text{acyl-iso-ma}}$  to form  $\text{trans}(\eta^2\text{-C}_3\text{H}_7\text{CO})\text{Co}(\text{CO})_2(\text{PBu}_3)$  **m**, in which the acyl group is at the axial site of the complex and has a  $\eta^2\text{-O}=\text{C}$  interaction at the equatorial site; iv) breaking the  $\eta^2\text{-O}=\text{C}$  interaction and adding  $\text{H}_2$  molecules with side-on orientation ( $\eta^2\text{-H}_2$ ) on the cobalt centre in **m** via  $\text{TS}_{\text{H}_2\text{-ma}}$  to obtain **[Co]-H<sub>2</sub>-a**; v) transformation from **[Co]-H<sub>2</sub>-a** to the less-stable complex **[Co]-H<sub>2</sub>-b** with the oxygen terminal of butyryl group towards the two equatorial carbonyl ligands through the rotation of the  $\text{Co}$ -butyryl  $\sigma$  bond (acyl rotation); vi) the formation of the  $\text{Co}(\text{III})$ -dihydride complex **[Co]-2H** via the splitting of  $\text{H}-\text{H}$  bond on the  $\text{Co}(\text{I})$  centre; vii) reductive elimination to form **[Co]-aldehyde** with weak  $\text{Co}\cdots\text{H}-\text{C}$  agostic interaction between the  $\text{Co}(\text{I})$  centre and the aldehyde product. The transformation pathway from **h** to the corresponding **[Co]-aldehyde** sequentially via the intermediates **j**, **l**, **n**, **[Co]-H<sub>2</sub>-a**, **[Co]-H<sub>2</sub>-b**, and **[Co]-2H** is

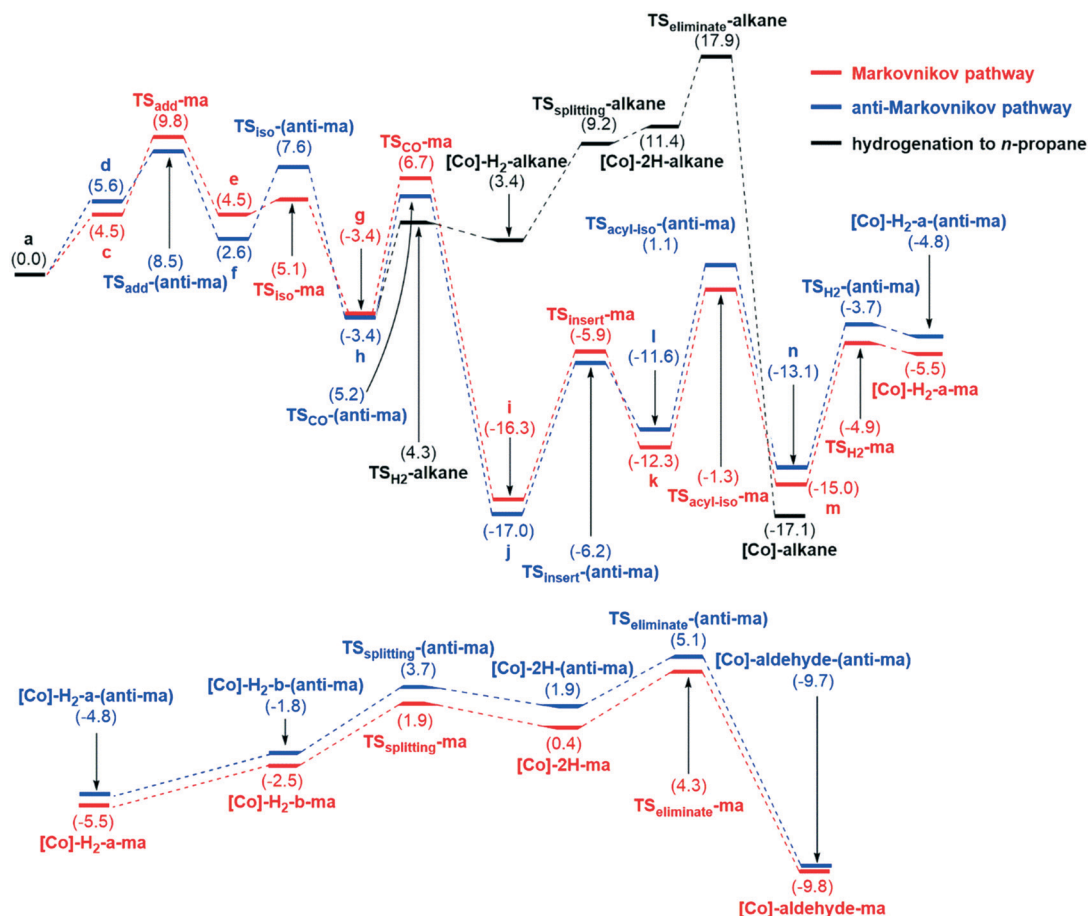


Fig. 5 Potential energy surface for the Markovnikov/anti-Markovnikov-type propene hydroformylation processes by the  $\text{PBu}_3$ -modified cobalt carbonyl catalyst.

analogous to the pathway illustrated in Fig. 4. The detailed results and structures for these four steps are given in Tables S5 and S6 in the ESI†. As shown in Fig. 5, the branched way and the linear way have very close reaction barriers for CO insertion (10.4 vs. 10.8 kcal mol<sup>-1</sup>), H<sub>2</sub> addition (10.1 vs. 9.4 kcal mol<sup>-1</sup>), H<sub>2</sub> splitting (4.4 vs. 5.5 kcal mol<sup>-1</sup>), and reductive elimination (3.2 vs. 3.9 kcal mol<sup>-1</sup>). Only in the hydrogen splitting step, the energy barrier of the branched way is 1.1 kcal mol<sup>-1</sup> lower than that of the linear way (4.4 vs. 5.5 kcal mol<sup>-1</sup>). The energy barrier for the isomerization of **k/l** to the more stable  $\eta^2\text{-O}=\text{C}$  coordinated **m/n** (12.7/11.0 kcal mol<sup>-1</sup>) is even higher than those for the CO-insertion and H<sub>2</sub> addition steps. The energy barriers of the hydrogen splitting and reductive elimination steps are all much lower than the activation energy for the addition of H<sub>2</sub> onto the cobalt centre of ( $\eta^2\text{-C}_3\text{H}_7\text{CO}$ )Co(CO)<sub>2</sub>(PBu<sub>3</sub>). This is also similar to that of the unmodified cobalt carbonyl catalyst, which suggests that H<sub>2</sub> coordination to the  $\eta^2\text{-O}=\text{C}$  acyl complexes is the rate-determining step in the stage of hydrogenolysis.

Summarizing the results of each individual step discussed above, the potential energy surface (PES) for propene hydroformylation by the  $\text{PBu}_3$ -modified cobalt carbonyl catalyst has been constructed and is displayed in Fig. 5.

Based on the above results, the rotation processes have relatively lower barrier than the other elementary steps and do not affect the rate-determining step as well as the whole reaction selectivity. For the clarity of PES and to facilitate the comparison, the corresponding energies of these rotation steps are omitted in Fig. 5 but are marked in the ESI† (Fig. S4 of ESI†). The whole reaction pattern is very similar to that of the unmodified cobalt carbonyl catalyst, which is suggested in a previous study.<sup>39</sup> The regioselectivity of the reaction product is mainly determined by the hydride transfer. The energy barriers for the addition of Co-H onto propene along the anti-Markovnikov pathway are lower than that along the Markovnikov pathway and the conversion from **a** to **f** is less endothermic than that from **a** to **e**. Compared with the PES for the processes from **a** to **e/f** on the unmodified cobalt carbonyl catalyst (Fig. S1 of ESI†), the relative free-energy difference of Co-H addition barriers between the Markovnikov and anti-Markovnikov pathways is significantly enlarged by using the  $\text{PBu}_3$ -modified cobalt carbonyl catalyst (1.3 vs. 0.2 kcal mol<sup>-1</sup>).

According to the calculated results, the ratio of linear to branched product in propene hydroformylation by  $\text{HCo}(\text{CO})_4$  is about 58:42, which is very close to the experimental result

of 57:43 reported by Tucci<sup>13</sup> but less than the result of 80:20 reported by Bourne *et al.*<sup>26,79</sup> When using  $\text{HCo}(\text{CO})_2(\text{PBU}_3)$  as the catalyst, the ratio is supposed to be 90:10, which fits very well with the experimental results of 89:11 (ref. 82) and 86:14.<sup>83</sup> It is obvious that phosphine ligand modified cobalt carbonyl catalyst considerably improved the regioselectivity of the linear product. Similar features were recently reported on Xantphos-doped Rh/POPs–PPh<sub>3</sub> hydroformylation catalyst.<sup>37</sup> The higher preference towards the linear product induced by the phosphine ligand than that by the carbonyl ligand has been demonstrated and the synchronous coordination of PPh<sub>3</sub> and Xantphos ligands has an even more remarkable effect on the linear selectivity of the products.

For isobutene hydroformylation by  $\text{HCo}(\text{CO})_4$ , the Markovnikov and anti-Markovnikov Co–H additions have close barriers (Fig. S2 in ESI<sup>†</sup>); therefore, the regioselectivity is thermodynamically controlled rather than being kinetically controlled. Based on the method proposed by Jiao *et al.*,<sup>39</sup> the ratio of the linear to the branched product could be estimated by the energy difference between the intermediates **i** and **j** (**i** is lower than **j** by about 1.1 kcal mol<sup>-1</sup>; for details, see Fig. S2<sup>†</sup>) at low temperature and the obtained 13:87 ratio is close to the experimental result of the Markovnikov addition selectivity reported by Heck *et al.*<sup>52</sup> However, at elevated temperature, the energy barrier difference of 0.3 kcal mol<sup>-1</sup> could be ignored and the anti-Markovnikov linear product could become dominant.<sup>12,80,81</sup>

### Cobalt-alkyl complexes hydrogenation

To further understand the chemical selectivity of alkane, the successive hydrogenation of *n*-propyl cobalt carbonyl complexes is also studied. On the  $\text{PBu}_3$ -modified catalyst, the process undergoes the following steps (Fig. 6): i) addition of H<sub>2</sub> onto the Co(I) centre (**h** → [Co]-H<sub>2</sub>-alkane); ii) generation of the Co(III)-dihydride complex *via* the cleavage of the H–H bond and the oxidation of the Co(I) centre ([Co]-H<sub>2</sub>-alkane → [Co]-2H-alkane); iii) regeneration of  $\text{HCo}(\text{CO})_2\text{L}$  and production of propane by reductive elimination ([Co]-2H-alkane → [Co]-alkane). The pathway of unmodified cobalt carbonyl catalyst requires the breaking of the agostic Co⋯H–

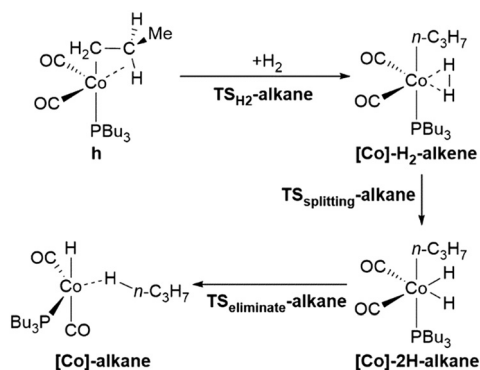


Fig. 6 Pathway of propene hydrogenation by the  $\text{PBu}_3$ -modified cobalt carbonyl catalyst.

C interaction in **f** by rotation of the propyl group at first (**f** → **o**) the detailed structural information is shown in Fig. S1<sup>†</sup>. The energy barriers and free energy changes in these elementary steps are listed in Table S7<sup>†</sup>.

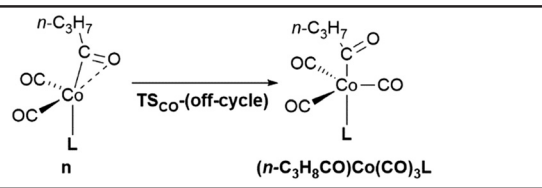
As shown in Fig. 5, starting from the intermediate **h**, the energy demand for hydrogenation of  $\text{Co}(\eta^2\text{-C}_3\text{H}_7)(\text{CO})_2(\text{PBU}_3)$  is 21.3 kcal mol<sup>-1</sup>, while the energy demand for CO insertion is only about 8.6 kcal mol<sup>-1</sup>. As shown in Fig. S1<sup>†</sup> regarding the unmodified catalyst, starting with the intermediate **f**, the energy demand for hydrogenation of  $\text{Co}(\eta^2\text{-C}_3\text{H}_7)(\text{CO})_3$  is 22.2 kcal mol<sup>-1</sup>, while the energy demand for CO insertion is only about 9.1 kcal mol<sup>-1</sup>. Obviously, the hydrogenation of *n*-propyl cobalt carbonyl complexes has considerably higher energy barriers than the migratory CO insertion both for  $\text{PBu}_3$ -modified and unmodified catalyst. It is indicated that the alkene has considerably lower selectivity than the aldehyde. Furthermore, the barrier difference between alkene formation and aldehyde formation is slightly lowered by  $\text{PBu}_3$  modification (13.1 vs. 12.7 kcal), which shows that the  $\text{PBu}_3$ -modified catalyst has higher alkene hydrogenation activity. The results agree well with the experimental report, *i.e.*, using the unmodified cobalt hydridocarbonyl catalyst, alkene hydrogenation is limited to 0.2 to 1.5% of the olefin feed,<sup>84</sup> while the ratio of alkene hydrogenation is elevated on the phosphine-modified cobalt hydridocarbonyl catalyst.<sup>84–88</sup>

Moreover,  $(\eta^1\text{-}n\text{-C}_3\text{H}_7\text{-CO})\text{Co}(\text{CO})_3\text{L}$  is the potential off-cycle intermediate in the cobalt-catalysed hydroformylation process. It is formed by CO coordination to cobalt centre of  $(\eta^2\text{-}n\text{-C}_3\text{H}_7\text{-CO})\text{Co}(\text{CO})_2\text{L}$ . As shown in Table 4, the process becomes more thermodynamically favoured by about 4.5 kcal mol<sup>-1</sup> when CO is substituted with  $\text{PBu}_3$ . A similar trend was also manifested in the CO coordination to the cobalt centre of  $(\eta^2\text{-}n\text{-C}_3\text{H}_7)\text{Co}(\text{CO})_2\text{L}$ . We, therefore, conclude that  $\text{PBu}_3$  can promote the CO addition or insertion on the cobalt-alkyl complexes.

### H<sub>2</sub> splitting and reductive elimination of the phosphine-modified cobalt carbonyl catalysts

To further understand the effect of phosphine ligand on the reaction reactivity to form the aldehyde, the hydrogen splitting and reductive elimination steps of other phosphine-modified cobalt carbonyl catalysts were also studied.

To make the computational results of different phosphine ligands comparable, the H<sub>2</sub>-attached complex [Co]-H<sub>2</sub>-a ( $(n\text{-C}_3\text{H}_7\text{CO})\text{Co}(\eta^2\text{-H}_2)(\text{CO})_2\text{L}$ ) with the butyryl group in the axial site was selected as the starting complex of H<sub>2</sub> splitting and reductive elimination process. The activation energies and reaction free energies of each step are listed in Table 5. More detailed free energy changes are given in Table S6<sup>†</sup>. The acquired results reveal two features about H<sub>2</sub> splitting and reductive elimination: i) replacing the carbonyl ligand at the axial site with the stronger electron-donating phosphine ligand significantly reduces the energy barrier of H<sub>2</sub> splitting on Co(I) by about 2–3 kcal mol<sup>-1</sup> and makes the H<sub>2</sub>-splitting step less endothermic by at least 2.4 kcal mol<sup>-1</sup>. As indicated

**Table 4** CO addition onto cobalt of  $(\eta^2\text{-}n\text{-C}_3\text{H}_7\text{CO})\text{Co}(\text{CO})_2\text{L}$ 


L	$\Delta G_A$	$\Delta G_R$
CO	5.7	-6.5
PBu <sub>3</sub>	6.8	-11.0

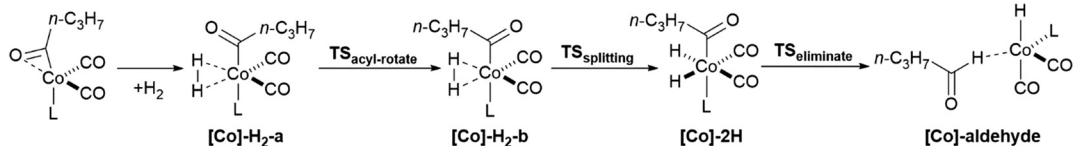
by Tolman electronic parameter,<sup>15,16</sup> these phosphine ligands have more  $\sigma$ -donor and less  $\pi$ -acid character than the carbonyl ligand, which leads to more  $\sigma$ -donation from the ligand to the Co(I) centre and less  $\pi$ -backdonation from the Co(I) centre to the empty ligand orbitals. This change makes the cobalt centre more electron-rich and more prone to oxidation by H<sub>2</sub>. Thus, phosphine ligand can effectively facilitate H<sub>2</sub> activation on Co(I) and stabilizes the Co(III)-dihydride complex; ii) for the transformation from [Co]-2H to [Co]-aldehyde, the elimination of aldehyde turns out to be a bit more difficult when the carbonyl ligand at the trans position of the butyryl group is replaced with the phosphine ligand. This is reflected on the elevated energy barrier and the less exergonic free energy change in the reductive elimination step. From these two features, we can see the distinct pros and cons of phosphine ligands on hydrogen activation and the following reductive elimination. Introducing the phosphine ligand is beneficial for the H-H bond cleavage on the cobalt catalyst but unfavourable for the last step of hydroformylation. It is noteworthy that among these four phosphine ligands, a<sub>5</sub>-PhobPC<sub>5</sub> exhibits impressive balance between H<sub>2</sub> splitting and reductive elimination. For H<sub>2</sub> splitting, the activation energy and reaction free energy on a<sub>5</sub>-PhobPC<sub>5</sub> are close to the other three phosphine ligands. However, for the reductive elimination step, a<sub>5</sub>-PhobPC<sub>5</sub> is more exothermic than the other three phosphine ligands by over 2 kcal mol<sup>-1</sup> (about 4 kcal mol<sup>-1</sup> more than PH<sub>3</sub> and PMe<sub>3</sub>). Referring to the results of PH<sub>3</sub>, PMe<sub>3</sub>, and PBu<sub>3</sub> with

relatively smaller Tolman cone angle, we deduce that the reductive elimination step benefits from the large Tolman cone angle of a<sub>5</sub>-PhobPC<sub>5</sub>. According to the kinetic investigation by Haynes *et al.*,<sup>24</sup> the cobalt-acyl complex containing a<sub>5</sub>-PhobPC<sub>5</sub> ligand has relatively high reactivity of hydrogenolysis. The obtained energy pattern of a<sub>5</sub>-PhobPC<sub>5</sub> for H<sub>2</sub> splitting and reductive elimination is consistent with these experimental results.

#### Further hydrogenation of aldehyde to alcohol as well as the reductive alkyloxycarbonylation of aldehyde to formic ester

In the previous reports, alcohol and formic ester are two kinds of side products obtained from the further reductive conversion of the hydroformylation product.<sup>84,89-91</sup> In particular, owing to the higher aldehyde hydrogenation activity, the proportion of alcohol and formic ester in the product mixture is increased in the reaction system with the phosphine-modified cobalt hydridocarbonyl catalyst.<sup>6,7,84,91</sup> Therefore, we further surveyed the reaction pathways of aldehyde hydrogenation to alcohol and carbonylative reduction to formic ester by employing *n*-butyraldehyde as the model substrate. Two Co-H addition modes were compared, as suggested in previous works.<sup>75,91</sup> The more favoured Co-H addition pathway *via* alkoxy cobalt intermediate<sup>92</sup> is discussed here and the other Co-H addition pathway *via* hydroxyalkyl cobalt<sup>93</sup> is listed in ESI† (Fig. S5 and S6) for comparison.

Similar to the formaldehyde and acyloin side-on coordination *via* formyl group to HCo(CO)<sub>3</sub> through the C=O  $\pi$  orbital,<sup>75,94</sup> HCo(CO)<sub>3</sub> and *n*-butyraldehyde can form the  $\pi$ -complex HCo( $\eta^2\text{-C}_3\text{H}_7\text{CHO}$ )(CO)<sub>3</sub>. There are also two orientations for the coordination of *n*-butyraldehyde's formyl group with the cobalt centre of HCo(CO)<sub>3</sub>: the C=O double bond is perpendicular or parallel to the axial Co-H bond.<sup>75,94</sup> The energy barrier for the transformation from perpendicular to parallel conformation *via* rotation is lower than 2 kcal mol<sup>-1</sup> and the free energy differences are rather small (for details about their structures and free energy comparison, see Table S8 in the ESI†). In these HCo( $\eta^2\text{-C}_3\text{H}_7\text{CHO}$ )(CO)<sub>3</sub>

**Table 5** Hydrogen splitting on  $(n\text{-C}_3\text{H}_7\text{CO})\text{Co}(\text{CO})_2\text{L}$  and reductive elimination of  $(n\text{-C}_3\text{H}_7\text{CO})\text{Co}(\eta^1\text{-H})_2(\text{CO})_2\text{L}$ 


Entry	L	$\Delta G_A(\text{acyl-rotate})$	$\Delta G_R(\text{acyl-rotate})$	$\Delta G_A(\text{splitting})$	$\Delta G_R(\text{splitting})$	$\Delta G_A(\text{eliminate})$	$\Delta G_R(\text{eliminate})$
1	CO	5.8	1.6	8.2	7.4	2.0	-14.3
2	PH <sub>3</sub>	6.7	3.2	5.1	4.1	2.6	-9.9
3	PMe <sub>3</sub>	6.1	1.7	6.3	5.0	3.6	-10.9
4	PBu <sub>3</sub>	7.4	3.0	5.5	3.7	3.2	-11.6
5	a <sub>5</sub> -PhobPC <sub>5</sub>	6.9	2.3	5.2	3.7	2.9	-13.8
6	PBu <sub>3</sub> <sup>a</sup>	6.7	3.0	4.4	2.9	3.9	-10.2

<sup>a</sup> i-C<sub>3</sub>H<sub>7</sub> instead of *n*-C<sub>3</sub>H<sub>7</sub>.

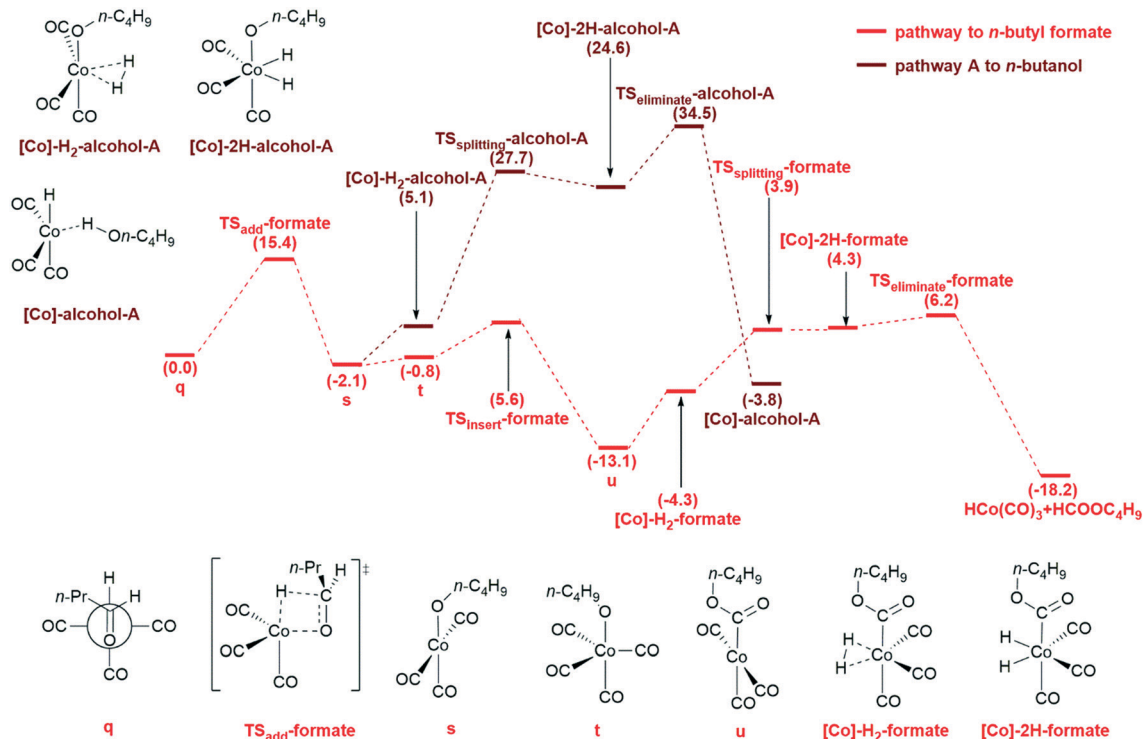


Fig. 7 Potential energy surface for *n*-butyraldehyde hydrogenation and carbonylative reduction by the cobalt hydridocarbonyl catalyst.

complexes, the oxygen atom of formyl group is much closer to the cobalt centre than the carbon atom by about 0.21 Å.

This phenomenon has been experimentally determined.<sup>95–97</sup> Distinct from the exothermic association between  $\text{HCo}(\text{CO})_3$

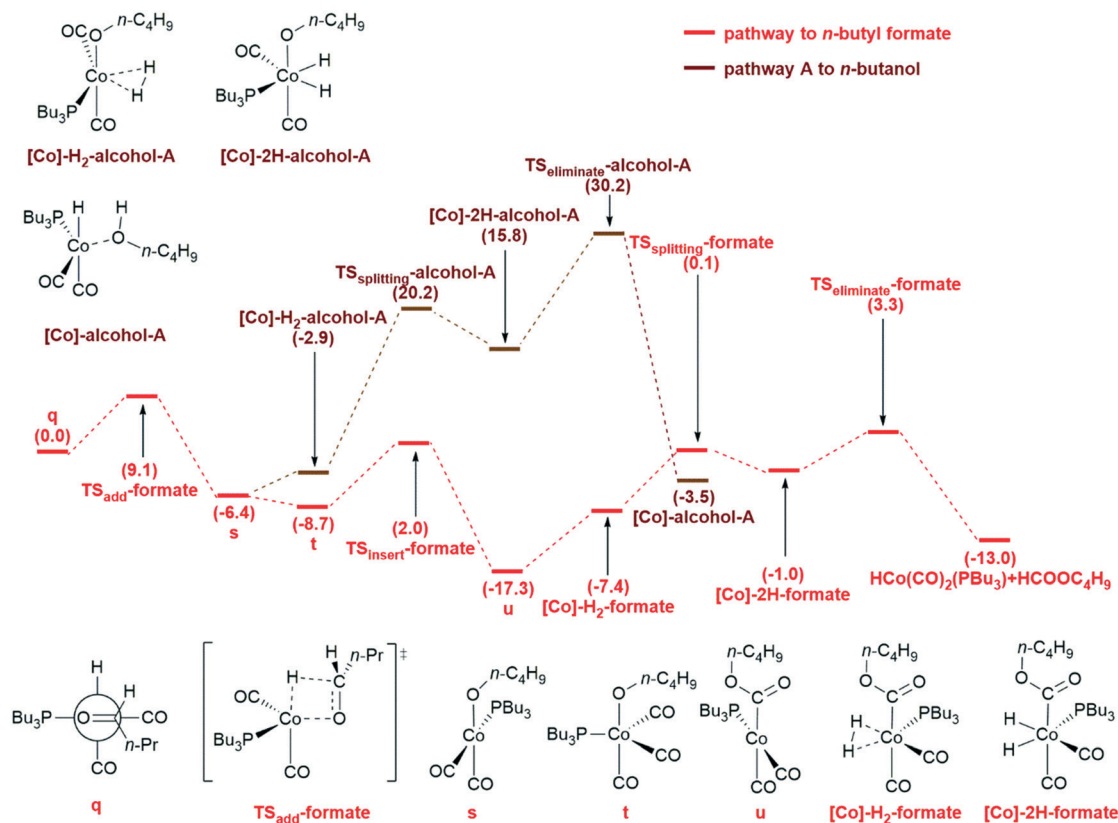


Fig. 8 Potential energy surface for *n*-butyraldehyde hydrogenation and carbonylative reduction by the  $\text{PBu}_3$ -modified cobalt hydridocarbonyl catalyst.

and the alkene, the coordination of *n*-butyraldehyde with  $\text{HCo}(\text{CO})_3$  is endothermic.

Fig. 7 depicts the PES of *n*-butyraldehyde hydrogenation and carbonylative reduction by the cobalt catalyst. As illustrated, Co–H addition is the rate-determining step ( $\mathbf{q} \rightarrow \mathbf{s}$ ,  $15.4 \text{ kcal mol}^{-1}$ ) for the formation of *n*-butyl formate. However, for the formation of alcohol,  $\text{H}_2$  splitting is the rate-determining step ( $[\text{Co}]\text{-2H-alcohol-B} \rightarrow [\text{Co}]\text{-alcohol-B}$ ,  $22.6 \text{ kcal mol}^{-1}$ ). For the  $\text{PBu}_3$ -modified catalyst, as shown in the PES (Fig. 8),  $\text{H}_2$  splitting is still the rate-determining step for alcohol formation ( $[\text{Co}]\text{-H}_2\text{-alcohol-B} \rightarrow [\text{Co}]\text{-2H-alcohol-B}$ ,  $23.1 \text{ kcal mol}^{-1}$ ), while CO insertion becomes the rate-determining step for *n*-butyl formate formation ( $\mathbf{t} \rightarrow \mathbf{u}$ ,  $10.7 \text{ kcal mol}^{-1}$ ). Comparing the whole process on the unmodified and  $\text{PBu}_3$ -modified catalyst (Fig. 7 and 8), the relative free energy of all the intermediates and the transition states involving the  $\text{HCo}(\text{CO})_2(\text{PBu}_3)$  catalyst was lower than that of the  $\text{HCo}(\text{CO})_3$  catalyst. Indeed, replacing the carbonyl ligand with phosphine ligand makes the formation of alcohol and formic ester easier. The results well explained the previous experimental phenomenon.

It should be mentioned that although the carbonylative reduction to *n*-butyl formate is both thermodynamically and kinetically favoured than the hydrogenation to alcohol, the detailed selectivity is also correlated with  $\text{CO}/\text{H}_2$  partial pressures, temperature, and other conditions,<sup>82,90,91</sup> currently, our computation results are unable to give quantitative preference of these two products.

## Conclusions

The steric and electronic effects of the phosphine ligand on the chemo-/regio-selectivity and reactivity of cobalt-based catalyst in hydroformylation have been systematically studied in this work. The computational results indicated the following patterns: i) for the hydroformylation of different terminal alkene substrates with unmodified cobalt carbonyl catalyst, only disubstituted alkene with bulky substitution groups can have good regioselectivity towards the linear product; ii) by introducing a phosphine ligand with large Tolman cone angle, the difference in the energy barrier of the Co–H addition step between the Markovnikov and anti-Markovnikov pathways turns out to be much more distinct than the unmodified cobalt carbonyl catalyst, which is more beneficial for the regioselectivity of hydroformylation towards the linear product; iii) replacing the carbonyl ligand with a relatively more electron-donating phosphine makes the process of  $\text{H}_2$  splitting step both kinetically and thermodynamically more favoured; however, the introduction of phosphine ligand has a negative impact on the reductive elimination step. Our computational investigation well-interprets the good regioselectivity towards the linear product of the  $\text{PBu}_3$ -modified cobalt carbonyl catalyst in the alkene hydroformylation. The potential energy surfaces for propene hydroformylation on the  $\text{PBu}_3$ -modified cobalt carbonyl catalyst illustrate that introducing the phosphine ligand does

not change the mechanism pattern and the linear regioselectivity of hydroformylation on the  $\text{PBu}_3$ -modified cobalt carbonyl catalyst is determined by the insertion of alkene into the Co–H bond during the beginning stage of the process.  $\text{PBu}_3$  modification on the catalyst can also alter the alkene chemoselectivity to a certain extent but the selectivity towards the alkane is still considerably lower than that towards the aldehyde. Furthermore, the subsequent alcohol and formic ester formation indeed have a great possibility. Our results provide important references for selecting the phosphine ligand to modify the cobalt-based catalysts and a bulky phosphine ligand is highly suggested to obtain higher regioselectivity of the linear product in hydroformylation.

## Conflicts of interest

There are no conflicts to declare.

## Acknowledgements

The work was financially supported by the National Natural Science Foundation of China (No. 21903049 and U1510103 for X.T., 21802151 for C.S., 91645118 and 21633013 for L.H.) and the Key Research Program of Frontier Sciences of CAS (QYZDJ-SSW-SLH051). Part of the calculations were performed at the Shanghai Supercomputing Centre and the Supercomputing Centre of Shanxi University.

## Notes and references

- 1 A. Behr and P. Neubert, *Applied Homogeneous Catalysis*, Wiley-VCH, Weinheim, Germany, 2012.
- 2 M. Taddei and A. Mann, *Hydroformylation for Organic Synthesis*, Springer-Verlag, Berlin-Heidelberg, 2013.
- 3 B. Cornils, A. Börner, R. Franke, B. Zhang, E. Wiebus and K. Schmid, *Applied Homogeneous Catalysis with Organometallic Compounds: A Comprehensive Handbook in Four Volumes*, Wiley-VCH, Weinheim, 3rd edn, 2017, ch. 2.
- 4 P. W. N. M. van Leeuwen and C. Claver, *Rhodium Catalyzed Hydroformylation*, Springer, Netherlands, 2002.
- 5 A. Börner and R. Franke, *Hydroformylation: Fundamentals, Processes, and Applications in Organic Synthesis*, Wiley-VCH, Weinheim, 2016.
- 6 R. Franke, D. Selent and A. Börner, *Chem. Rev.*, 2012, **112**, 5675–5732.
- 7 F. Hebrard and P. Kalck, *Chem. Rev.*, 2009, **109**, 4272–4282.
- 8 G. M. Torres, R. Frauenlob, R. Franke and A. Börner, *Catal. Sci. Technol.*, 2015, **5**, 34–54.
- 9 C. R. Greene and R. E. Meeker, *US Pat.*, 3274263, 1966.
- 10 L. H. Slaugh and R. D. Mullineaux, *US Pat.*, 3239569, 1966.
- 11 L. H. Slaugh and R. D. Mullineaux, *US Pat.*, 3239570, 1966.
- 12 L. H. Slaugh and R. D. Mullineaux, *J. Organomet. Chem.*, 1968, **13**, 469–477.
- 13 E. R. Tucci, *Ind. Eng. Chem. Prod. Res. Dev.*, 1968, **7**, 32–38.
- 14 W. Rupilius, J. J. McCoy and M. Orchin, *Product R&D*, 1971, **10**, 142–145.
- 15 C. A. Tolman, *J. Am. Chem. Soc.*, 1970, **92**, 2953–2956.

- 16 C. A. Tolman, *Chem. Rev.*, 1977, **77**, 313–348.
- 17 L. Perrin, E. Clot, O. Eisenstein, J. Loch and R. H. Crabtree, *Inorg. Chem.*, 2001, **40**, 5806–5811.
- 18 J. L. van Winkle, S. Lorenzo, R. C. Morris and R. F. Mason, *US Pat.*, 3420898, 1969.
- 19 C. Crause, L. Bennie, L. Damoense, C. L. Dwyer, C. Grove, N. Grimmer, W. J. van Rensburg, M. M. Kirk, K. M. Mokheseng, S. Otto and P. J. Steynberg, *Dalton Trans.*, 2003, 2036–2042.
- 20 A. Polas, J. D. E. T. Wilton-Ely, A. M. Z. Slawin, D. F. Foster, P. J. Steynberg, M. J. Green and D. J. Cole-Hamilton, *Dalton Trans.*, 2003, 4669–4677.
- 21 P. N. Bungu and S. Otto, *Dalton Trans.*, 2007, 2876–2884.
- 22 P. N. Bungu and S. Otto, *J. Organomet. Chem.*, 2007, **692**, 3370–3379.
- 23 P. N. Bungu and S. Otto, *Dalton Trans.*, 2011, **40**, 9238–9249.
- 24 J. M. Birbeck, A. Haynes, H. Adams, L. Damoense and S. Otto, *ACS Catal.*, 2012, **2**, 2512–2523.
- 25 Lim = 4,8-dimethyl-2-phosphabicyclo[3.3.1]nonane; VHC = mixture of 2-phosphabicyclo[3.3.1 and 3.2.2]nonane; PA = 1,3,5,7-tetramethyl-2,4,6-trioxa-8-phosphatricyclo[3.3.1.1.3,7]decane.
- 26 *New Syntheses with Carbon Monoxide*, ed. J. Falbe, Springer-Verlag, Berlin-Heidelberg, 1980, p. 39.
- 27 L. T. Mika, L. Orha, E. van Driessche, R. Garton, K. Zih-Perényi and I. T. Horváth, *Organometallics*, 2013, **32**, 5326–5332.
- 28 G. Achonduh, Q. Yang and H. Alper, *Tetrahedron*, 2015, **71**, 1241–1246.
- 29 Y. Shi, X. Hu, B. Zhu, S. Zhang and W. Huang, *Chem. Res. Chin. Univ.*, 2015, **31**, 851–857.
- 30 A. M. Kluwer, M. J. Krafft, I. Hartenbach, B. de Bruin and W. Kaim, *Top. Catal.*, 2016, **59**, 1787–1792.
- 31 S. S. Bhagade, S. R. Chaurasia and B. M. Bhanage, *Catal. Today*, 2018, **309**, 147–152.
- 32 X. Zhang, X. Tian, C. Shen, C. Xia and L. He, *ChemCatChem*, 2019, **11**, 1986–1992.
- 33 M. Torrent, M. Solà and G. Frenking, *Chem. Rev.*, 2000, **100**, 439–493.
- 34 T. Kégl, *RSC Adv.*, 2015, **5**, 4304–4327.
- 35 I. Jacobs, B. de Bruin and J. N. H. Reek, *ChemCatChem*, 2015, **7**, 1708–1718.
- 36 P. Dingwall, J. A. Fuentes, L. Crawford, A. M. Z. Slawin, M. Bühl and M. L. Clarke, *J. Am. Chem. Soc.*, 2017, **139**, 15921–15932.
- 37 C. Li, K. Sun, W. Wang, L. Yan, X. Sun, Y. Wang, K. Xiong, Z. Zhan, Z. Jiang and Y. Ding, *J. Catal.*, 2017, **353**, 123–132.
- 38 Y. Jiao, M. S. Torne, J. Gracia, J. W. Niemantsverdriet and P. W. N. M. van Leeuwen, *Catal. Sci. Technol.*, 2017, **7**, 1404–1414.
- 39 C.-F. Huo, Y.-W. Li, M. Beller and H. Jiao, *Organometallics*, 2003, **22**, 4665–4677.
- 40 J. P. Salinas-Olvera, R. M. Gómez and F. Cortés-Guzmán, *J. Phys. Chem. A*, 2008, **112**, 2906–2912.
- 41 C.-F. Huo, Y.-W. Li, M. Beller and H. Jiao, *Organometallics*, 2004, **23**, 765–773.
- 42 C.-F. Huo, Y.-W. Li, M. Beller and H. Jiao, *Organometallics*, 2005, **24**, 3634–3643.
- 43 C.-F. Huo, Y.-W. Li, M. Beller and H. Jiao, *Chem. – Eur. J.*, 2005, **11**, 889–902.
- 44 M. Solà and T. Ziegler, *Organometallics*, 1996, **15**, 2611–2618.
- 45 L. E. Rush, P. G. Pringle and J. N. Harvey, *Angew. Chem., Int. Ed.*, 2014, **53**, 8672–8676 (*Angew. Chem.*, 2014, **126**, 8816–8820).
- 46 E. N. Szlapa and J. N. Harvey, *Chem. – Eur. J.*, 2018, **24**, 17096–17104.
- 47 S. Maeda and K. Morokuma, *J. Chem. Theory Comput.*, 2012, **8**, 380–385.
- 48 S. Maeda, T. Taketsugu and K. Morokuma, *J. Comput. Chem.*, 2014, **35**, 166–173.
- 49 S. Habershon, *J. Chem. Phys.*, 2015, **143**, 094106.
- 50 S. Habershon, *J. Chem. Theory Comput.*, 2016, **12**, 1786–1798.
- 51 J. A. Varela, S. A. Vázquez and E. Martínez-Núñez, *Chem. Sci.*, 2017, **8**, 3843–3851.
- 52 R. F. Heck and D. S. Breslow, *J. Am. Chem. Soc.*, 1961, **83**, 4023–4027.
- 53 R. F. Heck, *Acc. Chem. Res.*, 1969, **2**, 10–16.
- 54 C. L. Dwyer, *Comprehensive Organometallic Chemistry III From Fundamentals to Applications*, 2007, vol. 1, pp. 483–507.
- 55 A. Haynes, *The Use of High Pressure Infrared Spectroscopy to Study Catalytic Mechanisms in Mechanisms in Homogeneous Catalysis. A Spectroscopic Approach*, ed. B. Heaton, Wiley-VCH, Weinheim, 2005, pp. 107–150.
- 56 C. Dwyer, H. Assumption, J. Coetzee, C. Crause, L. Damoense and M. Kirk, *Coord. Chem. Rev.*, 2004, **248**, 653–669.
- 57 L. Damoense, M. Datt, M. Green and C. Steenkamp, *Coord. Chem. Rev.*, 2004, **248**, 2393–2407.
- 58 P. C. J. Kamer, A. van Rooy, G. C. Schoemaker and P. W. N. M. van Leeuwen, *Coord. Chem. Rev.*, 2004, **248**, 2409–2424.
- 59 M. van Boven, N. H. Alemдарoglu and J. M. L. Penninger, *Product R&D*, 1975, **14**, 259–264.
- 60 M. van Boven, N. Alemдарoglu and J. M. L. Penninger, *J. Organomet. Chem.*, 1975, **84**, 65–74.
- 61 R. J. Klingler, M. J. Chen, J. W. Rathke and K. W. Kramarz, *Organometallics*, 2007, **26**, 352–357.
- 62 J. M. Dreimann, E. Kohls, H. F. W. Warmeling, M. Stein, L. F. Guo, M. Garland, T. N. Dinh and A. J. Vorholt, *ACS Catal.*, 2019, **9**, 4308–4319.
- 63 V. P. Ananikov, *Understanding Organometallic Reaction Mechanisms and Catalysis: Computational and Experimental Tools*, Wiley-VCH, Weinheim, 2014.
- 64 G.-J. Cheng, X. Zhang, L. W. Chung, L. Xu and Y.-D. Wu, *J. Am. Chem. Soc.*, 2015, **137**, 1706–1725.
- 65 Y. Zhao and D. Truhlar, *Theor. Chem. Acc.*, 2008, **120**, 215–241.
- 66 Y. Zhao and D. Truhlar, *Acc. Chem. Res.*, 2008, **41**, 157–167.
- 67 T. Sperger, I. A. Sanhueza, I. Kalvet and F. Schoenebeck, *Chem. Rev.*, 2015, **115**, 9532–9586.
- 68 M. Dolg, U. Wedig, H. Stoll and H. Preuss, *J. Chem. Phys.*, 1987, **86**, 866–872.

- 69 D. Andrae, U. Haussermann, M. Dolg, H. Stoll and H. Preuss, *Theor. Chem. Acc.*, 1990, **77**, 123–141.
- 70 L. Falivene, R. Credendino, A. Poater, A. Petta, L. Serra, R. Oliva, V. Scarano and L. Cavallo, *Organometallics*, 2016, **35**, 2286–2293.
- 71 M. J. Frisch, G. W. Trucks, H. B. Schlegel, G. E. Scuseria, M. A. Robb, J. R. Cheeseman, G. Scalmani, V. Barone, B. Mennucci, G. A. Petersson, H. Nakatsuji, M. Caricato, X. Li, H. P. Hratchian, A. F. Izmaylov, J. Bloino, G. Zheng, J. L. Sonnenberg, M. Hada, M. Ehara, K. Toyota, R. Fukuda, J. Hasegawa, M. Ishida, T. Nakajima, Y. Honda, O. Kitao, H. Nakai, T. Vreven, J. A. Montgomery, Jr., J. E. Peralta, F. Ogliaro, M. Bearpark, J. J. Heyd, E. Brothers, K. N. Kudin, V. N. Staroverov, R. Kobayashi, J. Normand, K. Raghavachari, A. Rendell, J. C. Burant, S. S. Iyengar, J. Tomasi, M. Cossi, N. Rega, J. M. Millam, M. Klene, J. E. Knox, J. B. Cross, V. Bakken, C. Adamo, J. Jaramillo, R. Gomperts, R. E. Stratmann, O. Yazyev, A. J. Austin, R. Cammi, C. Pomelli, J. W. Ochterski, R. L. Martin, K. Morokuma, V. G. Zakrzewski, G. A. Voth, P. Salvador, J. J. Dannenberg, S. Dapprich, A. D. Daniels, O. Farkas, J. B. Foresman, J. V. Ortiz, J. Cioslowski and D. J. Fox, *Gaussian 09, Revision D.01*, Gaussian, Inc., Wallingford CT, 2013.
- 72 A. Antolovic and E. R. Davidson, *J. Am. Chem. Soc.*, 1987, **109**, 5828–5840.
- 73 L. Versluis, T. Ziegler and L. Fan, *Inorg. Chem.*, 1990, **29**, 4530–4536.
- 74 S. Klaus, H. Neumann, H. Jiao, A. J. von Wangelin, D. Gördes, D. Strübing, S. Hübner, M. Hateley, C. Weckbecker, K. Huthmacher, T. Riermeier and M. Beller, *J. Organomet. Chem.*, 2004, **689**, 3685–3700.
- 75 C.-F. Huo, Y.-W. Li, M. Beller and H. Jiao, *Organometallics*, 2004, **23**, 2168–2178.
- 76 C.-F. Huo, Y.-W. Li, G.-S. Wu, M. Beller and H. Jiao, *J. Phys. Chem. A*, 2002, **106**, 12161–12169.
- 77 C.-F. Huo, T. Zeng, Y.-W. Li, M. Beller and H. Jiao, *Organometallics*, 2005, **24**, 6037–6042.
- 78 The terminal  $\nu(\text{CO})$  frequencies of  $(n\text{-C}_3\text{H}_7\text{CO})\text{Co}(\text{CO})_3(\text{PBu}_3)$  and  $(n\text{-C}_3\text{H}_7\text{CO})\text{Co}(\text{CO})_3(\text{a}_5\text{-PhobPC}_5)$  were compared in ref. 24.
- 79 R. V. Gholap, O. M. Kut and J. R. Bourne, *Ind. Eng. Chem. Res.*, 1992, **31**, 1597–1601.
- 80 I. Wender, J. Feldman, S. Metlin, B. H. Gwynn and M. Orchin, *J. Am. Chem. Soc.*, 1955, **77**, 5760–5761.
- 81 A. I. M. Keulemans, A. Kwantes and T. Van Bavel, *Rec. trav. chim.*, 1948, **67**, 298–308.
- 82 E. R. Tucci, *Ind. Eng. Chem. Prod. Res. Dev.*, 1968, **7**, 125–128.
- 83 F. Piacenti, M. Bianchi, E. Benedetti and P. Frediani, *J. Organomet. Chem.*, 1970, **23**, 257–264.
- 84 *New Syntheses with Carbon Monoxide*, ed. J. Falbe, Springer-Verlag, Berlin-Heidelberg, 1980, pp. 138–139.
- 85 J. Falbe, *J. Organomet. Chem.*, 1975, **94**, 213–227.
- 86 E. H. Pryde, E. N. Frankel and J. C. Cowan, *J. Am. Oil Chem. Soc.*, 1972, **49**, 451–456.
- 87 G. F. Pregaglia, A. Andretta, G. F. Ferrari and R. Ugo, *J. Organomet. Chem.*, 1971, **30**, 387–405.
- 88 L. Rosi, A. Bini, P. Frediani, M. Bianchi and A. Salvini, *J. Mol. Catal. A: Chem.*, 1996, **112**, 367–383.
- 89 C. L. Aldridge and H. B. Jonassen, *J. Am. Chem. Soc.*, 1963, **85**, 886–891.
- 90 C. D. Wood and P. E. Garrou, Phosphine Modified Cobalt Carbonyl Catalysts for the Hydroformylation of Dicyclopentadiene, in *Catalytic Conversions of Synthesis Gas and Alcohols to Chemicals*, ed. R. G. Herman, Springer, Boston, 1984.
- 91 C. D. Wood and P. E. Garrou, *Organometallics*, 1984, **3**, 170–174.
- 92 T. Bartik, T. Krümmeling, C. Krüger, L. Markó, R. Boese, G. Schmid, P. Vivarelli and G. Pályi, *J. Organomet. Chem.*, 1991, **421**, 323–333.
- 93 A. Sisak, E. Sámár-Szerencsés, V. Galamb and G. Pályi, *Organometallics*, 1989, **8**, 1096–1100.
- 94 L. Versluis and T. Ziegler, *J. Am. Chem. Soc.*, 1990, **112**, 6763–6768.
- 95 K. L. Brown, G. R. Clark, C. E. L. Headford, K. Marsden and W. R. Roper, *J. Am. Chem. Soc.*, 1979, **101**, 503–505.
- 96 S. Gambarotta, C. Floriani, A. Chiesi-Villa and C. Guastini, *J. Am. Chem. Soc.*, 1982, **104**, 2019–2020.
- 97 S. Gambarotta, C. Floriani, A. Chiesi-Villa and C. Guastini, *J. Am. Chem. Soc.*, 1985, **107**, 2985–2986.